
FORGET VECTORS AT PLAY: UNIVERSAL INPUT PERTURBATIONS DRIVING MACHINE UNLEARNING IN IMAGE CLASSIFICATION

A PREPRINT

Changchang Sun^{1*} Ren Wang² Yihua Zhang³ Jinghan Jia³
 Jiancheng Liu³ Gaowen Liu⁴ Sijia Liu³ Yan Yan¹
¹University of Illinois Chicago ²Illinois Institute of Technology
³Michigan State University ⁴Cisco Research

ABSTRACT

Machine unlearning (MU), which seeks to erase the influence of specific unwanted data from already-trained models, is becoming increasingly vital in model editing, particularly to comply with evolving data regulations like the “right to be forgotten”. Conventional approaches are predominantly model-based, typically requiring retraining or fine-tuning the model’s weights to meet unlearning requirements. In this work, we approach the MU problem from a novel input perturbation-based perspective, where the model weights remain intact throughout the unlearning process. We demonstrate the existence of a proactive input-based unlearning strategy, referred to *forget vector*, which can be generated as an input-agnostic data perturbation and remains as effective as model-based approximate unlearning approaches. We also explore *forget vector arithmetic*, whereby multiple class-specific forget vectors are combined through simple operations (*e.g.*, linear combinations) to generate new forget vectors for unseen unlearning tasks, such as forgetting arbitrary subsets across classes. Extensive experiments validate the effectiveness and adaptability of the forget vector, showcasing its competitive performance relative to state-of-the-art model-based methods. Codes are available at <https://github.com/Changchangsun/Forget-Vector>.

1 Introduction

To prevent unauthorized use of personal or sensitive data after training and comply with legislation such as the “right to be forgotten” (Hoofnagle et al., 2019), machine unlearning (MU) has garnered increasing attention as a solution to various challenges in vision tasks (Golatkar et al., 2020; Poppi et al., 2023; Warnecke et al., 2021; Fan et al., 2023). In essence, it initiates a reverse learning process to erase the impact of unwanted data (*e.g.*, specific data points, classes, or knowledge concepts) from an already-trained model, while still preserving its utility for information not targeted by an unlearning request. Based on the guarantees provided for data removal from already-trained models, existing MU methods can be broadly categorized into two approaches: *exact unlearning* (Dong et al., 2024; Guo et al., 2019; Thudi et al., 2022b) and *approximate unlearning* (Graves et al., 2021; Thudi et al., 2022a; Becker & Liebig, 2022; Izzo et al., 2021). Exact unlearning guarantees the complete and verifiable removal of targeted data, typically achieved by retraining the model from scratch with the data to be forgotten excluded from the training set, a process we refer to as Retrain. However, due to the high computational overhead and lack of scalability of exact unlearning, research has increasingly focused on approximate unlearning methods, which seek to achieve efficient unlearning without requiring full retraining.

Approximate unlearning strikes a balance between computational efficiency and effective data removal, making it practical for many real-world applications. Most existing approximate unlearning techniques are *model-based*, updating the model’s weights within a limited number of training iterations to eliminate the influence of specific unwanted data, thus avoiding a full retraining process. Representative methods in this category include fine-tuning approaches (Warnecke et al., 2021; Perifanis et al., 2024), gradient ascent techniques (Thudi et al., 2022a; Chen et al., 2024a), and influence function-based methods (Golatkar et al., 2021, 2020). Although these model-based unlearning

*Work conducted during the visit to the OPTML Group@Michigan State University.

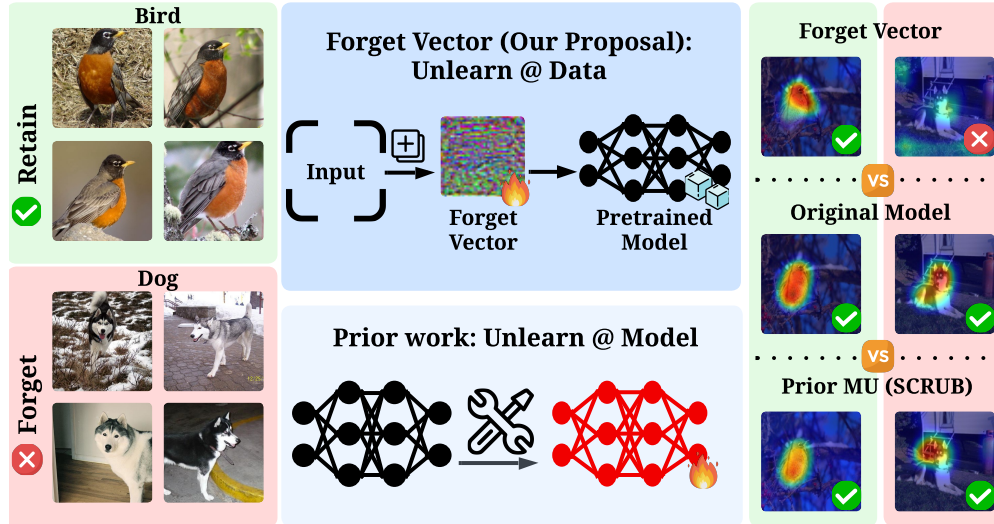


Figure 1: A schematic illustration comparing our proposed data-based MU method (termed the ‘forget vector’), which achieves unlearning objectives (*i.e.*, forgetting ‘dog’ and remembering ‘bird’ in this example) by operating directly on input data without altering model parameters, against traditional model update-based unlearning methods. ✖ indicates that the forget data is successfully unlearned, while ✔ means that the forget data was *not* successfully unlearned, or the retain data was correctly recognized. The ‘original model’ refers to the model without unlearning applied, and ‘SCRUB’ (Kurmanji et al., 2024b) represents an existing unlearning method that updates model weights.

methods have made significant strides, they often overlook the *data-based* dimension and its potential impact on MU. For instance, it remains unclear whether current MU approaches generalize effectively to ‘shifted’ forget data, produced by external perturbations. Additionally, the possibility of a data-based MU design that operates without updating model parameters has yet to be explored. Therefore, this work aims to take a step forward in addressing the following research question:

(Q) Can we explore data influence in MU and harness data-based operations to fulfill MU?

To address (Q), we study MU from a fresh data-based viewpoint: **forget vector**, a universal input data perturbation designed to promote unlearning effectively; See the schematic overview in Fig. 1. Before developing the forget vector, we explore the rationale for how data-based perturbations complement current model-based MU approaches, as evidenced by these methods’ generalization to common data shifts, including Gaussian noise and adversarial perturbations (Hendrycks & Dietterich, 2019; Goodfellow et al., 2014). Our design for the forget vector is also related to recent input prompting techniques for vision models, known as visual prompting (Bahng et al., 2022b; Chen et al., 2023; Oh et al., 2023) or model reprogramming (Elsayed et al., 2018; Zhang et al., 2022; Chen, 2024), used in transfer learning and model adaptation. These prompting methods learn input perturbations to enable a fixed model to perform well on new tasks, effectively guiding the model to execute tasks it wasn’t originally trained for. From this perspective, our research on the forget vector also explores whether it is possible to append a trainable ‘prompt’ to the input to guide an already-trained neural network in unlearning specific data. We summarize **our contributions** below.

- We investigate the impact of forget data shifts on image classifiers post-unlearning, revealing that unlearning demonstrates resilience against these shifts (to some extent) while generalization remains more vulnerable.
- Building on the complementary role of data shifts in MU, we propose a proactive, input-agnostic data perturbation strategy termed the *forget vector*, optimized specifically to facilitate unlearning.
- We demonstrate the effectiveness of *forget vector arithmetic* by using class-wise forget vectors to generate new vectors that effectively eliminate the influence of specific data subsets in image classification models.
- We conduct extensive experiments on MU for image classification, providing both quantitative and qualitative analyses to demonstrate the competitiveness of the forget vector compared to model-based MU methods.

2 Related Work

MU in Vision. Machine unlearning (MU) in vision has gained significant attention due to the increasing need for privacy preservation, copyright protection, and ethical data removal in machine learning models. Recent studies (Wang et al., 2024b; Pan et al., 2022; Li et al., 2024a; Foster et al., 2024; Lin et al., 2023; Gupta et al., 2021; Kurmanji et al.,

2024b; Di et al., 2022; Chen et al., 2024b; Zhang et al., 2024b; Liu et al., 2024a) in this area have primarily focused on two main tasks: image generation and image classification. For image generation, MU techniques (Fan et al., 2023; Li et al., 2024a; Zhang et al., 2024b) have been proposed to prevent models from generating unwanted or harmful content while retaining high-quality outputs. For example, weight saliency methods guide MU by identifying and selectively altering model parameters to eliminate specific content generation (Fan et al., 2023). In image classification, MU methods have explored various approaches to effectively erase certain classes or images from models (Thudi et al., 2022a; Chen et al., 2024a; Golatkar et al., 2020, 2021; Liu et al., 2024a; Pochinkov & Schoots, 2024). Specifically, fine-tuning-based methods update the model incrementally on a modified dataset without the unwanted data points (Warnecke et al., 2021; Perifanis et al., 2024). Gradient ascent-based approaches attempt to reverse the impact of unwanted data by applying gradient ascent to the model parameters (Thudi et al., 2022a; Chen et al., 2024a). Influence-based unlearning techniques estimate the impact of specific data points on model predictions and parameters, and then reverse those contributions to achieve unlearning (Golatkar et al., 2020, 2021). Another line of research investigates the relationship between MU and model pruning, suggesting that model sparsity can help to bridge the gap between approximate and exact unlearning, reducing the need for complex parameter updates (Liu et al., 2024a; Pochinkov & Schoots, 2024). However, most existing MU methods for vision are model-based, often leading to utility degradation after unlearning and incurring high computational costs.

Beyond vision, MU has been applied to other domains, with notable efforts in natural language processing (Shi et al., 2024; Wang et al., 2024a, 2023a; Liu et al., 2024b), graph-based data (Li et al., 2024b; Dong et al., 2024), and time-series data (Du et al., 2019).

Input-based Model Adaptation. This approach has gained attention as an effective method to modify or repurpose pre-trained models for new tasks or specific objectives without the need for full retraining. It is particularly beneficial for reducing computational costs and leveraging the existing knowledge within models. Key techniques in model adaptation include: Visual prompting (Jia et al., 2022; Wang et al., 2023b; Liu et al., 2023; Hossain et al., 2024; Zhang et al., 2024a) maintains the pre-trained model’s parameters fixed and adapts the input to enable the model to perform different tasks. For example, introducing trainable parameters in the input space while keeping the model backbone frozen can achieve comparable results with reduced computational overhead. Model reprogramming (Tsai et al., 2020; Elsayed et al., 2018; Yang et al., 2021; Melnyk et al., 2023) involves keeping a pre-trained model unchanged while modifying its inputs to adapt the model for new tasks. For example, adversarial perturbations can be applied to inputs at test time, allowing the model to perform a specific task dictated by the perturbations, even if that task was not originally intended for the model. Feature-based domain adaptation (Wang et al., 2018; Tahmoresnezhad & Hashemi, 2017) applies transformations or mapping techniques to the input data, aligning the feature distributions between the source and target domains while keeping the model unchanged.

3 Preliminaries on MU and Problem Statement

In this section, we introduce the fundamentals of machine unlearning (MU), including its formulation, commonly-used methods, and evaluation metrics, and motivate our focus: an data-based forget vector design for achieving MU.

Formulation of MU. In this work, we focus on the problem of MU for image classification. Let $\mathcal{D} = \{\mathbf{x}_i, y_i\}_{i=1}^N$ represent a training set with N examples, where \mathbf{x}_i denotes the i th image data, and y_i denotes its corresponding class label. We introduce a *forget set* $\mathcal{D}_f \subseteq \mathcal{D}$, which specifies the training samples targeted for unlearning. Accordingly, the complement of \mathcal{D}_f is the *retain set*, i.e., $\mathcal{D}_r = \mathcal{D} \setminus \mathcal{D}_f$. The *goal of MU* is to efficiently and effectively eliminate the influence of \mathcal{D}_f on an already-trained model θ , so that the performance of the post-unlearning model closely approximates that of a model retrained from scratch on \mathcal{D}_r (i.e., excluding the impact of \mathcal{D}_f from scratch). Therefore, such a retraining method (referred to as *Retrain*) is typically considered as the gold standard of MU (Thudi et al., 2022a; Jia et al., 2023). However, since Retrain is computationally intensive, most popular MU approaches instead address an unlearning optimization problem using the forget and retain sets to update the model parameters θ , starting from the originally pre-trained model, denoted by θ_o . This yields the following optimization problem for MU:

$$\underset{\theta}{\text{minimize}} \quad \ell_{\text{MU}}(\theta; \mathcal{D}_f, \mathcal{D}_r), \quad (1)$$

with the initialization $\theta = \theta_o$. In (1), ℓ_{MU} represents an appropriate unlearning loss function that may depend on \mathcal{D}_f and/or \mathcal{D}_r , as will be detailed when introducing specific unlearning methods. In the context of MU for image classification (Golatkar et al., 2020; Fan et al., 2023), the specification of the forget set \mathcal{D}_f leads to two unlearning scenarios: *class-wise forgetting*, where \mathcal{D}_f consists of a subset focused on a specific image class targeted for unlearning, and *random data forgetting*, where \mathcal{D}_f is a randomly selected subset of images across all classes.

Model Update-based MU Methods and Evaluation. The formulation in (1) represents the predominant MU solution in the literature, focusing on modifying model weights and/or architectural components to achieve the unlearning objective.

In what follows, we introduce several representative MU approaches that serve as approximations to Retrain. (a) Fine-tuning (**FT**) (Warnecke et al., 2021): This approach treats the MU problem as a continual learning task, defining the unlearning objective ℓ_{MU} as a training objective that fine-tunes θ over \mathcal{D}_r to induce catastrophic forgetting of \mathcal{D}_f . (b) Random labeling (**RL**) (Golatkar et al., 2020): This approach specifies the unlearning objective ℓ_{MU} by assigning random labels or features to the data in \mathcal{D}_f , thereby enforcing model forgetting. (c) Gradient ascent (**GA**) (Thudi et al., 2022a): This approach employs the negative of the FT loss to reverse the training impact associated with the data in \mathcal{D}_f . (d) Localization-informed unlearning (Jia et al., 2023; Fan et al., 2023): This method identifies a subset of model weights critical to the unlearning task (e.g., through model sparsity (Jia et al., 2023) or gradient saliency (Fan et al., 2023)) and incorporates this weight localization as a prior to solve the unlearning problem in (1).

Given an unlearned model (denoted as θ_u) after solving (1), unlearning performance is evaluated in two main areas: *unlearning effectiveness*, which measures whether the target data/information has been successfully removed, and *utility retention*, which assesses whether unlearning has preserved the model’s classification ability on unaffected data. Following the evaluation benchmark in (Jia et al., 2023), unlearning effectiveness can be quantified by two metrics: unlearning accuracy (**UA**), defined as $1 - \text{the model’s accuracy on } \mathcal{D}_f$ (higher UA indicates better unlearning), and membership inference attack performance on \mathcal{D}_f , termed **MIA-Efficacy**, where higher prediction accuracy on non-training samples indicates better unlearning. Utility retention is measured by retain accuracy (**RA**), reflecting the model’s accuracy on \mathcal{D}_r , and testing accuracy (**TA**), which is the accuracy on the original test set.

Data-based MU Design: The Forget Vector Problem. While previous MU approaches can be unified within the framework of (1) by varying the unlearning loss ℓ_{MU} and weight localization priors, recent advancements in input data-based model adaptation, such as visual prompting (Bahng et al., 2022a; Chen et al., 2023) and model reprogramming (Chen, 2024; Elsayed et al., 2018), suggest an alternative approach to MU. This strategy inspires us to design data-based prompting (implemented through universal input perturbations) to achieve unlearning without modifying the model itself. We refer to this input perturbation vector, designed specifically for MU, as the **forget vector**. To be more specific, let δ represent the data-agnostic input perturbations to be designed. The problem of constructing a forget vector for MU can be formulated as

$$\underset{\delta}{\text{minimize}} \quad \ell_{\text{MU}}(\delta; \theta_o, \mathcal{D}_f, \mathcal{D}_r), \quad (2)$$

where δ is the perturbation variable, applied linearly to the forget samples as $\mathbf{x}' := \mathbf{x} + \delta$ for $\mathbf{x} \in \mathcal{D}_f$, similar to visual prompting (Bahng et al., 2022a) and adversarial examples (Goodfellow et al., 2014). Unlike model-based MU methods, we will detail the unlearning objective function required for designing the forget vector in our later method sections.

To address (2), we are motivated to explore two research questions: **(Q1)** How do “perturbations” applied to forget data affect unlearning performance? **(Q2)** How can we effectively design the forget vector δ to solve problem (2)? These two questions are interconnected: the answer to (Q1) offers a sensitivity analysis of MU to data shifts within the forget set, guiding how the specific shift induced by the forget vector can be optimized for effective unlearning in (Q2). Therefore, the following Secs. 4-5 address (Q1) and (Q2) in sequence. For (Q1), the next section analyzes performance through an evaluation lens on a given unlearned model, using data perturbations applied via standard data augmentation techniques or adversarial perturbations.

4 Generalization of MU to Forget Data Shifts

Before designing the forget vector as formulated in (2), we examine the sensitivity of existing model-based unlearning approaches to external perturbations applied to forget data. Such a perturbation-based or out-of-distribution (OOD) generalization analysis of MU has not been explored in the literature. Our rationale is that if conventional MU approaches demonstrate robustness to these external forget data perturbations post unlearning, then enhancing MU with a forget vector could become a seamless process, as a proactive design of such a vector would likely yield effective results.

Post-unlearning Forget Data Perturbations. Given an unlearned model (θ_u) after solving (1), we examine two types of shifts in forget data: standard data corruptions used in the evaluation of OOD generalization (Hendrycks et al., 2021; Hendrycks & Dietterich, 2019) and worst-case perturbations generated by adversarial attacks (Goodfellow et al., 2014; Madry et al., 2017).

(a) *Data Corruptions.* Following the OOD generalization evaluation approach in image classification (Hendrycks et al., 2021; Hendrycks & Dietterich, 2019), we introduce data corruptions from four main categories: noise, blur, weather,

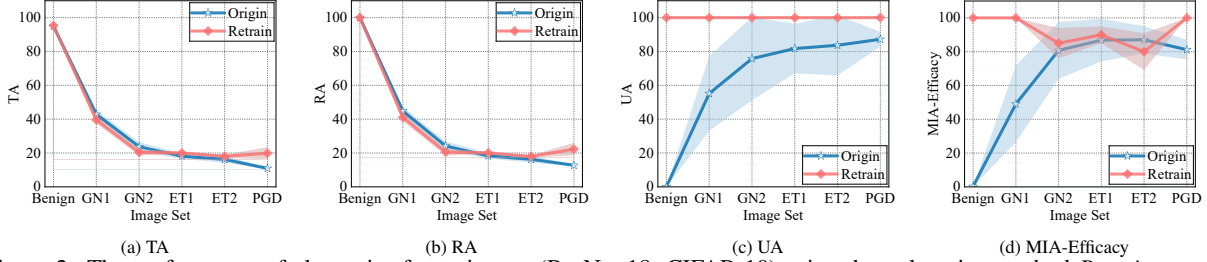


Figure 2: The performance of class-wise forgetting on (ResNet-18, CIFAR-10) using the unlearning method *Retrain* vs. the (pre-unlearning) original model performance (Origin), evaluated on both benign evaluation sets (Benign) and perturbed sets, which include (1) Gaussian noise (GN) with a standard deviation of 0.08 (termed GN1), (2) GN with a standard deviation of 0.2 (termed GN2), (3) Elastic transformation (ET) with parameters (488, 170.8, 24.4) regarding intensity, smoothing, and offset (termed ET1), (4) ET with parameters (488, 19.52, 48.8) (termed ET2), and (5) adversarial perturbations from a 7-step PGD attack with strength $\epsilon = 8/255$. The unlearning performance metrics are reported as (a) TA (testing accuracy), (b) RA (retain accuracy), (c) UA (unlearning accuracy), and (d) MIA-Efficacy, as defined in Sec. 3. The average performance is reported over 10 independent trials, where each trial focuses on forgetting one specific class from CIFAR-10. Shaded regions indicate the performance variance.

and digital. Each type of corruption includes five levels of severity, with higher levels representing increased noise intensity. Among these, we select zero-mean Gaussian noise (GN) and Elastic transformations (ET) as the primary corruption types to evaluate MU robustness against shifts in forget data. Our rationale is that Gaussian noise yields small pixel-wise perturbations (similar to adversarial perturbations introduced later) and Elastic transformations stretch or contract small image regions.

(b) *Adversarial perturbations.* An adversarial image is a benign image altered with carefully crafted, pixel-wise perturbations designed to mislead a classifier. In this work, we use the ϵ -constrained ℓ_∞ norm-based K -step projected gradient descent (PGD) attack (Goodfellow et al., 2014; Madry et al., 2017) to generate adversarial examples via iterative projected gradient updates. The parameter $\epsilon > 0$ defines the radius of the ℓ_∞ norm of the perturbations, controlling their strength. And K represents the number of PGD steps.

Generalization of MU to Forget Data Perturbations. Next, we apply the above data shift operations to the MU evaluation sets—namely, the forget, retain, and testing sets—and assess the unlearning performance of an unlearned model. Fig. 2 displays the performance of the gold standard unlearning method, Retrain, against Gaussian noise at test time with standard deviations of 0.08 and 0.2 (Hendrycks & Dietterich, 2019), and two types of Elastic transformations with parameters (488, 170.8, 24.4) and (488, 19.52, 48.8) regarding intensity, smoothing and offset for moderate and high-intensity distortions (Hendrycks & Dietterich, 2019), as well as a 7-step PGD attack with perturbation strength $\epsilon = 8/255$ (Goodfellow et al., 2014). To ensure the feasibility of Retrain, we conduct the image classification task using ResNet-18 on the CIFAR-10 dataset.

As shown in Fig. 2-(a) and (b), model utility, measured by RA (retain accuracy) and TA (testing accuracy), decreases when external perturbations are applied to the evaluation sets compared to its original performance without perturbations. This is expected due to the generalization loss when facing data shifts. More interestingly, Fig. 2-(c) and (d) show that unlearning effectiveness of Retrain, measured by UA (unlearning accuracy) and MIA-Efficacy, remains stable despite the presence of these perturbations on the forget set. This is because perturbations degrade prediction performance across evaluation sets, including the forget set. This is further evidenced by the increase in UA and MIA-Efficacy for the original model (without unlearning) when exposed to data perturbations. The above indicates that a reduction in prediction performance on the forget set could translate into enhanced unlearning effectiveness on that set. In Appendix A, we provide additional evaluations of other approximate unlearning methods, including FT, RL, and GA, showing consistent performance.

The results above demonstrate that unlearning effectiveness is inherently preserved under external perturbations at no additional cost. However, balancing this with utility retention in the presence of perturbations remains challenging. Therefore, we need to address the forget vector problem (2) to develop an input-based MU solution that enhances unlearning effectiveness without compromising model utility.

5 Optimization for Forget Vectors

As motivated in Sec. 4, if we treat the forget vector as an external perturbation applied to the forget set, our goal becomes optimizing its design to maximize unlearning effectiveness without compromising the original model utility. To this end, we first propose an unlearning objective function, ℓ_{MU} , tailored for the forget vector design in (2), inspired by the untargeted C&W attack (Carlini & Wagner, 2017). We then introduce a novel paradigm called compositional

unlearning, facilitated by forget vector arithmetic. These approaches center on optimizing the input perturbation δ in (2) while keeping the model unchanged, *i.e.*, identical to the pre-trained original model $\theta = \theta_o$.

Unlearning Objective Design of Forget Vectors. Our design aims for the forget vector variable (δ), when applied to the forget set (\mathcal{D}_f), to drive the model’s predictions (θ_o) away from the correct labels. Conversely, when applied to the retain set (\mathcal{D}_r), the forget vector should minimally affect correct predictions. The first forget objective aligns with adversarial attack design, aiming to mislead the model’s predictions in the presence of the perturbation δ . The second retain objective acts as a utility regularization, suppressing the unlearning effect of the perturbation when applied to data samples not targeted for unlearning.

To implement the forget objective (denoted by ℓ_f), we draw inspiration from the C&W untargeted attack loss (Carlini & Wagner, 2017). This is given by a margin loss, designed to remain active when the top prediction matches the correct label, ensuring that optimization continues until predictions are shifted to an incorrect label, thereby achieving unlearning. This yields

$$\ell_f(\delta; \theta_o, \mathcal{D}_f) = \mathbb{E}_{(\mathbf{x}, y) \in \mathcal{D}_f} \max\{f_{\theta_o, y}(\mathbf{x} + \delta) - \max_{k: k \neq y} f_{\theta_o, k}(\mathbf{x} + \delta), -\tau\}, \quad (3)$$

where $(\mathbf{x}, y) \in \mathcal{D}_f$ denotes a forget sample with y being the true label of \mathbf{x} , $\mathbf{x} + \delta$ is the perturbed sample, $f_{k, \theta_o}(\mathbf{x})$ denotes the prediction logit (before softmax) of the model θ_o for class k under the input \mathbf{x} , and $\tau \geq 0$ is a margin threshold that controls the unlearning strength. The rationale behind (3) is that minimizing it ensures convergence to the negative margin $f_y(\mathbf{x} + \delta) - \max_{k \neq y} f_k(\mathbf{x} + \delta) \rightarrow -\tau \leq 0$. Thus, the forget vector δ enforces unlearning on θ for \mathbf{x} by making the incorrect prediction ($k \neq y$) have a higher confidence than the original correct prediction y . On the other hand, once the margin becomes negative (indicating that the prediction label has been flipped), the forget objective ℓ_f automatically terminates, allowing a balance with the retain objective, which will be introduced later. In our experiments, we find that the forget objective is robust to variations in the *nonnegative* margin parameter τ (see Appendix B). A larger τ value imposes a stricter unlearning requirement by increasing the logit distance from the correct label. For example, we set $\tau = 1$ in our experiments.

Next, we regularize the forget objective (3) with the retain objective, defined as the cross-entropy loss (ℓ_{CE}) over the retain set \mathcal{D}_r , along with the ℓ_2 norm of δ to ensure minimal perturbation required to achieve both the forget and retain objectives. This yields the full unlearning objective in (2):

$$\ell_{MU}(\delta; \theta_o, \mathcal{D}_f, \mathcal{D}_r) = \ell_f(\delta; \theta_o, \mathcal{D}_f) + \lambda_1 \ell_{CE}(\delta; \theta_o, \mathcal{D}_r) + \lambda_2 \|\delta\|_2^2, \quad (4)$$

where $\lambda_1 > 0$ and $\lambda_2 > 0$ are the regularization parameters, and $\ell_{CE}(\delta; \theta_o, \mathcal{D}_r)$ denotes the CE loss of the model θ_o over the perturbed retain set $\{(\mathbf{x} + \delta, y)\}_{(\mathbf{x}, y) \in \mathcal{D}_r}$. Integrating (4) into (3), we can then apply stochastic gradient descent (SGD) (Amari, 1993) to optimize the forget vector variable δ .

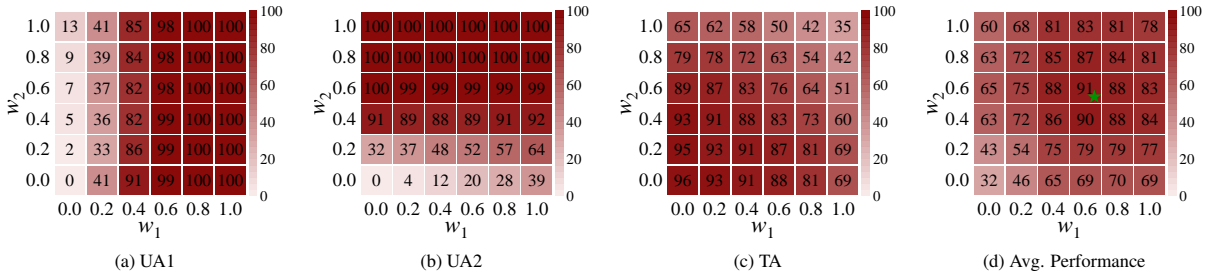


Figure 3: The performance of forget vector arithmetic regarding class 1 and class 2 on CIFAR-10 with ResNet-18 evaluated across different combination coefficients w_1 and w_2 ranging from 0 to 1 with an interval of 0.2, includes (1) unlearning accuracy for class 1 (UA1), (2) unlearning accuracy for class 2 (UA2), (3) testing accuracy for remaining classes (TA), and (4) the average (avg.) performance across UA1, UA2, and TA, with a green star (★) marking the optimized weight scheme (w_1 and w_2) that minimizes (4) over \mathbf{w} in (5). The color bar on the right represents a gradient scale from light to dark red, indicating the range of values (0 to 100%) in the heatmap. The integer within each cell represents the performance (%) given a combination of w_1 and w_2 .

Compositional Unlearning via Forget Vector Arithmetic. A forget vector defines an unlearning direction in the input space to guide the unlearning process. We explore whether a *new* unlearning direction can be efficiently constructed by interpolating from existing forget vectors, such as class-wise forget vectors obtained by solving (4) with \mathcal{D}_f defined as each class’s training set. This approach is analogous to the concept of task vectors in weight space for model editing (Ilharco et al., 2022). However, to the best of our knowledge, *input-based* task vector arithmetic has not yet been explored in the literature. If forget vectors can be modified and combined using arithmetic operations, such as negation and addition, we can dynamically adjust a model’s unlearning behavior without re-solving the optimization problem (4) or any other model-based unlearning problem in (1). We refer to this new unlearning paradigm as *compositional unlearning*.

Let δ_k denote the forget vector used for unlearning data points of class k . Given the set of forget vectors $\{\delta_k\}_{k=1}^K$ for all K classes, we obtain these vectors by solving (4) with \mathcal{D}_f defined as each class’s training set, respectively. The forget vector for compositional unlearning is given by

$$\delta(\mathbf{w}) := \sum_{k=1}^K (w_k \delta_k), \quad (5)$$

where $\mathbf{w} = [w_1, \dots, w_K]^K$ are the linear combination coefficients to be optimized, which determine the forget vector arithmetic. To determine \mathbf{w} , we can minimize (4) with the optimization restricted to the coefficients \mathbf{w} . Instead of penalizing the ℓ_2 norm of the forget vector, we penalize the ℓ_2 norm of \mathbf{w} to prevent excessive pixel perturbation. This modifies (4) to the problem $\min_{\mathbf{w}} \ell_f(\delta(\mathbf{w}); \theta_o, \mathcal{D}_f) + \lambda_1 \ell_{CE}(\delta(\mathbf{w}); \theta_o, \mathcal{D}_r) + \lambda_2 \|\mathbf{w}\|_2^2$. As will be shown later, random data forgetting can be achieved through class-wise forget vector arithmetic (5) by applying the compositional scheme defined by the coefficients \mathbf{w} .

To illustrate the effectiveness of forget vector arithmetic, **Fig. 3** shows preliminary results of combining two class-wise forget vectors (δ_1 and δ_2) using a simple scheme $\delta(\mathbf{w}) = w_1 \delta_1 + w_2 \delta_2$ on (CIFAR-10, ResNet-18). Rather than optimizing \mathbf{w} , we adjust its value and observe changes in unlearning accuracy for image class 1 (UA1) and for class 2 (UA2), as well as TA (testing accuracy) for the remaining classes, as w varies. As shown in Fig. 3-(a) and (b), higher UA1 and UA2 values occur with increased w_1 or w_2 , indicating a positive impact on unlearning performance for classes 1 and 2. Additionally, Fig. 3-(c) reveals that TA remains relatively stable under moderate weighting. These results suggest that more aggressive weighting of forget vectors enhances unlearning for the target classes but may negatively impact testing accuracy for other classes. An optimal weighting scheme can be identified by minimizing problem (4) over \mathbf{w} using (5). This is supported by the average performance shown in Fig. 3-(d), where the highest average performance aligns closely with the optimized weighting scheme marked by the green star (★).

6 Experiments

6.1 Experiment Setups

Datasets and Models. We focus on MU for image classification, using two datasets: CIFAR-10 (Krizhevsky et al., 2009) and ImageNet-10, a 10-class subset of the original ImageNet (Deng et al., 2009), for ease of implementation of Retrain (exact unlearning) over ImageNet images as (Huang et al., 2022; Tao et al., 2021). For these tasks, we use two well-trained image classifiers: ResNet-18 (He et al., 2016) for CIFAR-10 and VGG-16 (Simonyan & Zisserman, 2014) for ImageNet-10 classification.

Unlearning Baselines and Evaluations. In the context of MU for image classification, we consider two scenarios: *class-wise forgetting* and *data-wise forgetting*. In class-wise forgetting, training data from an image class are designated for unlearning, while in random data forgetting, a subset of all-class training points is randomly selected as the forget set, with a specified forget ratio of 10%. To demonstrate the effectiveness of our proposal, we consider 6 MU baseline methods, including ① FT (Warnecke et al., 2021), ② RL (Golatkhar et al., 2020), ③ GA (Thudi et al., 2022a), ④ NegGrad+ (Kurmanji et al., 2024a), ⑤ SalUn (Fan et al., 2023), and ⑥ SCRUB (Kurmanji et al., 2024b).

As described in Sec. 3, unlearning effectiveness is measured using UA (unlearning accuracy) and MIA-Efficacy, while model utility post-unlearning is assessed by RA (retain accuracy) and TA (testing accuracy); for all metrics, higher values indicate better performance. It is also worth noting that all existing model-based MU baseline methods ①-⑥ are evaluated on non-perturbed evaluation sets. However, when using our proposed data-based forget vector solution, we need to perturb the evaluation sets (including the forget set, retain set, and testing set) through the forget vector to assess unlearning effectiveness and utility retention.

To quantify the performance gap with Retrain, we compare each unlearning baseline and our proposal against this exact unlearning method across all metrics. We report an averaged assessment, termed *Averaging (Avg.) Gap*. Unless specified otherwise, all the main experiments (whether class-wise or random data forgetting) are conducted over 10 random trials, with mean performance reported.

Implementation Details of Our Proposal. To solve the forget vector problem (2) with the proposed unlearning objective in (4), we set the retain loss regularization parameter λ_1 to 3 for CIFAR-10 and 5 for ImageNet-10 in class-wise forgetting, and to 1 for random data forgetting. The ℓ_2 -norm regularization parameter is set to $\lambda_2 = 1$. These hyperparameters are determined through a grid search over the range $[0, 10]$. To optimize (2), we use stochastic gradient descent (SGD) (Amari, 1993) with a momentum factor of 0.9 and an exponential learning rate scheduler, decaying at a rate of 0.9 per iteration. Additionally, the batch size is set to 256, with a maximum of 40 optimization iterations for both two datasets. To solve the compositional unlearning problem (5), we use a similar setup, setting both λ_1 and λ_2 to 1.

6.2 Experiment Results

Table 1: Performance overview of various MU methods for image classification under two unlearning scenarios on CIFAR-10 and ImageNet-10 using ResNet-18 and VGG-16, respectively. Results are reported in the format $a \pm b$, where a is the mean and b denotes standard deviation b over 10 independent trials. The performance gap against Retrain is indicated in (\bullet), where a lower value is better. \uparrow (or \downarrow) indicates that a higher (or lower) value is better. The best performance for each metric is highlighted in **green**, while the second-best performance is highlighted in **red**.

MU Method	UA \uparrow	MIA-Efficacy \uparrow	RA \uparrow	TA \uparrow	Avg.Gap \downarrow	UA \uparrow	MIA-Efficacy \uparrow	RA \uparrow	TA \uparrow	Avg.Gap \downarrow
Class-wise Forgetting, CIFAR-10						Class-wise Forgetting, ImageNet-10				
Retrain	100.00 \pm 0.00(0.00)	100.00 \pm 0.00(0.00)	99.91 \pm 0.03(0.00)	94.92 \pm 0.15(0.00)	0.00	100.00 \pm 0.00(0.00)	100.00 \pm 0.00(0.00)	99.66 \pm 0.16(0.00)	97.11 \pm 0.82(0.00)	0.00
FT	5.27 \pm 0.73(94.73)	51.49 \pm 5.07(48.51)	100.0 \pm 0.0(0.09)	95.03 \pm 0.07(0.14)	35.86	39.66 \pm 4.73(60.34)	55.76 \pm 7.26(44.24)	99.78 \pm 0.03(0.13)	97.27 \pm 0.35(2.35)	26.77
RL	18.87 \pm 7.34(81.13)	98.94 \pm 0.79(1.06)	99.98 \pm 0.0(0.07)	94.51 \pm 0.12(0.41)	20.67	76.58 \pm 11.64(23.42)	46.04 \pm 33.71(53.96)	99.28 \pm 0.2(0.63)	96.91 \pm 0.55(1.99)	20.00
GA	71.45 \pm 0.35(28.55)	81.7 \pm 0.22(18.30)	98.62 \pm 0.04(1.29)	92.34 \pm 0.02(2.58)	12.68	46.61 \pm 6.11(53.39)	49.15 \pm 9.36(50.85)	99.35 \pm 0.11(0.56)	95.6 \pm 0.22(0.68)	26.37
NegGrad+	91.78 \pm 14.66(8.22)	95.81 \pm 7.28(4.19)	98.35 \pm 1.22(1.56)	92.62 \pm 1.34(2.3)	4.07	49.56 \pm 34.87(50.44)	64.27 \pm 27.33(35.73)	99.08 \pm 1.18(0.58)	96.47 \pm 1.25(0.64)	21.84
SalUn	96.35 \pm 2.14(3.65)	98.64 \pm 0.03(1.36)	98.75 \pm 0.18(1.16)	92.34 \pm 1.54(2.58)	2.19	95.13 \pm 1.79(4.87)	97.24 \pm 0.17(2.76)	96.33 \pm 0.25(3.33)	96.18 \pm 1.10(0.93)	2.97
SCRUB	93.45 \pm 2.33(6.55)	96.38 \pm 1.72(3.62)	99.95 \pm 0.0(0.04)	94.56 \pm 0.07(0.36)	2.64	99.12 \pm 0.14(0.89)	98.01 \pm 0.51(1.09)	99.75 \pm 0.03(0.09)	97.24 \pm 0.16(0.13)	0.77
Ours	97.88 \pm 0.27(2.12)	99.60 \pm 0.15(0.41)	97.25 \pm 0.24(2.66)	90.90 \pm 0.32(4.02)	2.30	87.23 \pm 6.55(12.77)	91.41 \pm 5.9(8.59)	94.77 \pm 1.16(5.14)	94.04 \pm 1.29(0.88)	6.85
Random Data Forgetting, CIFAR-10						Random Data Forgetting, ImageNet-10				
Retrain	5.50 \pm 0.16(0.00)	11.57 \pm 0.47(0.00)	99.88 \pm 0.05(0.00)	94.24 \pm 0.19(0.00)	0.00	4.05 \pm 0.45(0.00)	6.60 \pm 1.07(0.00)	99.48 \pm 0.07(0.00)	96.33 \pm 0.38(0.00)	0.00
FT	0.03 \pm 0.03(5.47)	0.75 \pm 0.09(10.82)	99.98 \pm 0.02(0.10)	94.45 \pm 0.14(0.21)	4.15	1.35 \pm 0.32(2.70)	4.67 \pm 1.61(1.93)	99.36 \pm 0.28(0.12)	96.54 \pm 0.59(0.21)	1.24
RL	0.52 \pm 0.24(4.98)	3.13 \pm 0.55(8.44)	99.85 \pm 0.07(0.03)	93.88 \pm 0.20(0.36)	3.45	2.96 \pm 0.42(1.09)	12.85 \pm 4.25(0.25)	99.19 \pm 0.16(0.29)	95.50 \pm 0.9(0.83)	2.12
GA	1.56 \pm 0.08(3.94)	2.88 \pm 2.44(8.69)	98.67 \pm 2.74(1.21)	92.84 \pm 2.59(1.40)	3.81	0.18 \pm 0.04(3.87)	2.97 \pm 1.51(3.63)	99.88 \pm 0.01(0.38)	97.47 \pm 0.09(1.14)	2.23
NegGrad+	0.97 \pm 0.05(3.57)	2.74 \pm 2.16(8.83)	99.42 \pm 0.87(0.46)	93.38 \pm 1.13(0.86)	3.67	0.60 \pm 0.44(3.45)	3.90 \pm 2.22(2.70)	99.68 \pm 0.28(0.20)	97.12 \pm 0.45(0.79)	1.79
SalUn	1.73 \pm 0.25(4.77)	6.25 \pm 1.21(5.32)	99.24 \pm 0.09(0.64)	91.03 \pm 1.13(3.21)	3.23	1.15 \pm 0.40(2.90)	3.56 \pm 1.12(3.04)	98.97 \pm 1.56(0.51)	95.42 \pm 2.10(0.91)	1.84
SCRUB	0.61 \pm 0.31(4.89)	3.69 \pm 0.54(7.88)	99.76 \pm 0.18(0.12)	93.91 \pm 0.19(0.33)	3.31	0.18 \pm 0.08(3.87)	2.80 \pm 1.33(3.80)	99.88 \pm 0.03(0.41)	97.36 \pm 0.15(1.03)	2.28
Ours	2.61 \pm 0.46(2.81)	8.26 \pm 1.17(3.49)	97.33 \pm 0.47(2.55)	90.97 \pm 0.38(3.27)	2.92	2.27 \pm 0.50(1.78)	6.13 \pm 1.40(0.47)	98.29 \pm 0.32(1.19)	95.82 \pm 0.48(0.51)	0.99

Overview Performance of Forget Vector. In **Tab. 1**, we compare the performance of our forget vector approach with other model-based MU methods across the metrics: UA, RA, TA, MIA-Efficacy, and Avg. Gap vs. Retrain. We highlight two key observations below. **First**, in terms of unlearning effectiveness (UA and MIA-Efficacy), the data perturbation-based forget vector demonstrates highly competitive performance compared to model update-based MU baselines, typically ranking among the top two methods with the smallest performance gap relative to Retrain. The advantage of the forget vector is particularly evident in MIA-Efficacy, where it achieves the closest results to Retrain. **Second**, in terms of model utility post-unlearning (RA and TA), the forget vector generally leads to a larger performance drop than other methods. This is not surprising, as the forget vector introduces data perturbations to the retain and testing tests at evaluation while keeping the model unchanged, even though it is designed to preserve model utility in (4). Nonetheless, a certain RA or TA loss may still occur. However, considering the gain in unlearning effectiveness, the Avg. Gap with Retrain shows that the forget vector remains competitive, ranking among the top two unlearning methods. Furthermore, we remark that the utility loss caused by the forget vector could be mitigated by refraining from applying it to utility datasets, as its primary role is to proactively enforce forgetting on the forget set.

Table 2: Unlearning accuracy (%) of forget vector transferred to unseen forget sets under 3 scenarios on (CIFAR-10, ResNet-18).

MU Method	D'_f	D'_f	D'_f
	from testing class	perturbed by GN1	perturbed by ET1
Retrain	100.00 \pm 0.00(0.00)	64.73 \pm 3.36(0.00)	81.43 \pm 0.28(0.00)
FT	21.44 \pm 1.11(78.56)	56.75 \pm 1.40(7.98)	81.79 \pm 0.18(0.36)
RL	27.90 \pm 5.7(72.10)	61.84 \pm 2.45(2.89)	81.15 \pm 0.20(0.28)
GA	73.95 \pm 0.6(26.05)	55.20 \pm 2.59(9.53)	82.17 \pm 0.76(1.28)
NegGrad+	93.86 \pm 10.93(6.14)	57.81 \pm 1.76(6.92)	81.73 \pm 0.65(0.30)
SalUn	97.55 \pm 1.37(2.45)	73.15 \pm 4.25(8.42)	80.27 \pm 3.56(1.16)
SCRUB	93.65 \pm 2.65(6.35)	61.95 \pm 0.86(1.85)	81.18 \pm 0.62(0.25)
Ours	98.26 \pm 0.35(1.74)	78.32 \pm 1.03(13.59)	85.03 \pm 0.91(3.60)

Transferability of Forget Vector to Unseen Forget Data. Conventionally, unlearning effectiveness is typically measured on the original forget set (D_f). However, with the data perturbation-based forget vector, it is also interesting to investigate its unlearning transferability when applied to a new, previously unseen forget set (denoted as D'_f) that share similarities with D_f and are equally appropriate for unlearning. In the context of class-wise forgetting, we consider D'_f using the testing data from the class targeted for unlearning. In the context of data forgetting, we obtain D'_f by applying the data corruption operation GN1 and ET1 used in **Fig. 2** to perturb D_f . **Tab. 2** shows the UA of the forget vector applied to the unseen forget set D'_f . As observed, the unlearning performance of the forget vector remains effective when evaluated on D'_f . Among the model update-based unlearning baselines, current SOTA methods such as SCRUB (Kurmanji et al., 2024b) and SalUn (Fan et al., 2023) also demonstrate generalization to D'_f , compared to simpler MU methods like FT, RL, and GA, which show lower transferability, as evidenced in the class-wise forgetting on (CIFAR-10, ResNet-18).

Table 3: Compositional unlearning on CIFAR-10 and ImageNet-10, where FV represents the forget vector in the original random-data forgetting scenario, and CU-FV denotes compositional unlearning achieved via pre-learned class-wise forget vector arithmetic.

MU Method	UA \uparrow	RA \uparrow	TA \uparrow	MIA-Efficacy \uparrow	Avg.Gap \downarrow
CIFAR-10					
Retrain	5.50 \pm 0.16(0.00)	11.57 \pm 0.47(0.00)	99.88 \pm 0.05(0.00)	94.24 \pm 0.19(0.00)	0.00
FV	2.61 \pm 0.49(2.89)	8.26 \pm 1.17(3.00)	97.33 \pm 0.47(2.55)	90.97 \pm 0.38(3.27)	2.92
CU-FV	5.36 \pm 0.60(0.14)	9.76 \pm 0.91(1.81)	94.93 \pm 0.64(4.95)	88.60 \pm 0.59(5.64)	3.16
ImageNet-10					
Retrain	4.05 \pm 0.45(0.00)	6.60 \pm 1.07(0.00)	99.48 \pm 0.07(0.00)	96.33 \pm 0.38(0.00)	0.00
FV	2.27 \pm 0.50(1.78)	6.13 \pm 1.40(0.47)	98.29 \pm 0.32(1.19)	95.82 \pm 0.48(0.51)	0.99
CU-FV	2.27 \pm 1.18(0.00)	4.95 \pm 1.86(1.18)	97.93 \pm 1.09(0.36)	91.41 \pm 1.25(4.41)	1.49

Compositional Unlearning by Class-wise Forget Vectors. Next, we demonstrate the effectiveness of compositional unlearning via forget vector arithmetic (termed CU-FV). Using class-wise forget vectors, we apply their linear combination as defined in (5) to achieve random data forgetting. **Tab. 3** compares the performance of CU-FV with Retrain (the exact unlearning method) and the direct forget vector approach (FV) applied to the targeted forget set. Interestingly, we observe that CU-FV achieves the overall performance comparable to FV, as indicated by similar Avg. Gap values. Unlike FV, CU-FV optimizes only the class-wise coefficients in (5), resulting in a much smaller optimization space than FV. However, from UA and MIA-Efficacy metrics, we find that unlearning effectiveness is easier to maintain since unlearning typically targets a smaller subset of data points. In contrast, model utility (RA and TA) may decline more with CU-FV than with FV. This is possibly because retention across a larger set of data points unrelated to unlearning requires a higher level of optimization to preserve model utility effectively.

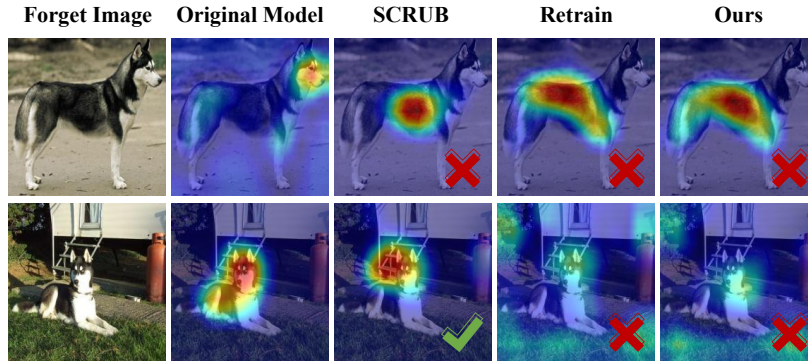


Figure 4: Gradient-based saliency map visualized via Grad-CAM for different MU methods against **forget images**. The highlighted areas (marked in red) indicate regions most influential to model prediction, and the red cross mark (✗) indicates that corresponding methods effectively unlearn the input forget images while the check (✓) signifies the opposite.

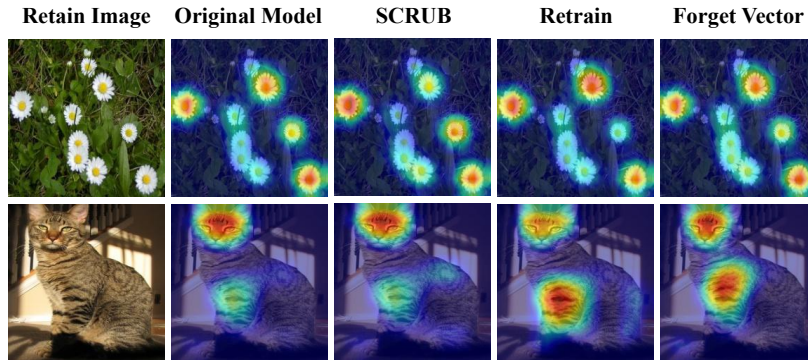


Figure 5: Gradient-based saliency map visualization using Grad-CAM for different MU methods against **retain images**.

Assessing Forget Vector via An Input Saliency Lens. In **Figs. 4** and **5**, we explore the impact of the forget vector on unlearning and utility retention through input saliency map, using Grad-CAM (Gradient-weighted Class Activation Mapping) (Bengio et al., 2013). Using Grad-CAM, we visualize the salient pixels (*i.e.*, regions most influential

to model prediction) for both forget and retain images under different unlearning scenarios: (1) the original model (without unlearning), (2) Retrain, (3) SCRUB-based unlearning, and (4) forget vector-based unlearning. In the first three scenarios, we obtain the input saliency maps on raw forget/retain images without the addition of the forget vector, while in the last scenario, the input saliency is applied to images perturbed by the forget vector. As seen in **Fig. 4**, only the forget vector and Retrain methods effectively unlearn the target input images, evident from the significant shifts in saliency regions compared to those in the original model. In contrast, the MU baseline SCRUB shows minimal saliency shifts, failing to adequately forget the target data in the last two rows. On the other hand, when evaluating input saliency on retain data in **Fig. 5**, we observe that the forget vector and other unlearning methods produce input saliency maps similar to those of the original model, indicating retained saliency for non-forgotten images. Moreover, we provide additional visualization results in Appendix D.

Ablation Studies. In Appendix C, we provide additional ablation studies on the sensitivity of the unlearning-retaining regularization parameter λ_1 in (4) and compare the runtime costs of forget vector calculation with those of other model-based unlearning methods.

7 Conclusion and Limitations

In this paper, we introduced a novel, data-based approach to machine unlearning (MU) in image classification, termed the *forget vector*. Unlike traditional model-based MU methods that require retraining or fine-tuning model weights, our approach shows that input-agnostic data perturbations can effectively achieve unlearning objectives. Our method demonstrates competitive performance relative to model-based approximate unlearning techniques. Furthermore, we showcase the potential of compositional unlearning: new forget vectors for unseen tasks, such as unlearning arbitrary subsets across classes, can be generated through simple arithmetic operations, like linear combinations of class-specific forget vectors. Extensive experiments confirm the effectiveness and adaptability of our optimized forget vector.

While effective, the forget vector approach relies on input perturbations, which may not be fully robust against white-box adversarial attacks that are aware of the forget vector strategy. Additionally, compositional unlearning’s dependence on pre-trained class-wise forget vectors could increase computational costs in cases where obtaining these vectors is challenging. Future work could focus on improving the robustness of forget vectors and developing more computationally efficient arithmetic techniques for compositional unlearning.

References

- Shun-ichi Amari. Backpropagation and stochastic gradient descent method. *Neurocomputing*, 5(4-5):185–196, 1993.
- Hyojin Bahng, Ali Jahanian, Swami Sankaranarayanan, and Phillip Isola. Exploring visual prompts for adapting large-scale models. *arXiv preprint arXiv:2203.17274*, 2022a.
- Hyojin Bahng, Ali Jahanian, Swami Sankaranarayanan, and Phillip Isola. Visual prompting: Modifying pixel space to adapt pre-trained models. *arXiv preprint arXiv:2203.17274*, 3(11-12):3, 2022b.
- Alexander Becker and Thomas Liebig. Evaluating machine unlearning via epistemic uncertainty. *arXiv preprint arXiv:2208.10836*, 2022.
- Yoshua Bengio, Nicholas Léonard, and Aaron Courville. Estimating or propagating gradients through stochastic neurons for conditional computation. *arXiv preprint arXiv:1308.3432*, 2013.
- Nicholas Carlini and David Wagner. Towards evaluating the robustness of neural networks. In *2017 IEEE Symposium on Security and Privacy (SP)*, pp. 39–57. Ieee, 2017.
- Aochuan Chen, Yuguang Yao, Pin-Yu Chen, Yihua Zhang, and Sijia Liu. Understanding and improving visual prompting: A label-mapping perspective. In *Proceedings of the IEEE/CVF Conference on Computer Vision and Pattern Recognition*, pp. 19133–19143, 2023.
- Kongyang Chen, Zixin Wang, Bing Mi, Waixi Liu, Shaowei Wang, Xiaojun Ren, and Jiaying Shen. Machine unlearning in large language models. *arXiv preprint arXiv:2404.16841*, 2024a.
- Pin-Yu Chen. Model reprogramming: Resource-efficient cross-domain machine learning. In *Proceedings of the AAAI Conference on Artificial Intelligence*, volume 38, pp. 22584–22591, 2024.
- Ruizhe Chen, Jianfei Yang, Huimin Xiong, Jianhong Bai, Tianxiang Hu, Jin Hao, Yang Feng, Joey Tianyi Zhou, Jian Wu, and Zuozhu Liu. Fast model debias with machine unlearning. *Advances in Neural Information Processing Systems*, 36, 2024b.
- Jia Deng, Wei Dong, Richard Socher, Li-Jia Li, Kai Li, and Li Fei-Fei. Imagenet: A large-scale hierarchical image database. In *2009 IEEE conference on computer vision and pattern recognition*, pp. 248–255. Ieee, 2009.

- Jimmy Z Di, Jack Douglas, Jayadev Acharya, Gautam Kamath, and Ayush Sekhari. Hidden poison: Machine unlearning enables camouflaged poisoning attacks. In *NeurIPS ML Safety Workshop*, 2022.
- Yushun Dong, Binchi Zhang, Zhenyu Lei, Na Zou, and Jundong Li. Idea: A flexible framework of certified unlearning for graph neural networks. In *Proceedings of the 30th ACM SIGKDD Conference on Knowledge Discovery and Data Mining*, pp. 621–630, 2024.
- Min Du, Zhi Chen, Chang Liu, Rajvardhan Oak, and Dawn Song. Lifelong anomaly detection through unlearning. In *Proceedings of the 2019 ACM SIGSAC conference on computer and communications security*, pp. 1283–1297, 2019.
- Gamaleldin F Elsayed, Ian Goodfellow, and Jascha Sohl-Dickstein. Adversarial reprogramming of neural networks. *arXiv preprint arXiv:1806.11146*, 2018.
- Chongyu Fan, Jiancheng Liu, Yihua Zhang, Dennis Wei, Eric Wong, and Sijia Liu. Salun: Empowering machine unlearning via gradient-based weight saliency in both image classification and generation. *arXiv preprint arXiv:2310.12508*, 2023.
- Jack Foster, Stefan Schoepf, and Alexandra Brintrup. Loss-free machine unlearning. *arXiv preprint arXiv:2402.19308*, 2024.
- Aditya Golatkar, Alessandro Achille, and Stefano Soatto. Eternal sunshine of the spotless net: Selective forgetting in deep networks. In *Proceedings of the IEEE/CVF Conference on Computer Vision and Pattern Recognition*, pp. 9304–9312, 2020.
- Aditya Golatkar, Alessandro Achille, Avinash Ravichandran, Marzia Polito, and Stefano Soatto. Mixed-privacy forgetting in deep networks. In *Proceedings of the IEEE/CVF conference on computer vision and pattern recognition*, pp. 792–801, 2021.
- Ian J Goodfellow, Jonathon Shlens, and Christian Szegedy. Explaining and harnessing adversarial examples. *arXiv preprint arXiv:1412.6572*, 2014.
- Laura Graves, Vineel Nagisetty, and Vijay Ganesh. Amnesiac machine learning. In *Proceedings of the AAI Conference on Artificial Intelligence*, volume 35, pp. 11516–11524, 2021.
- Chuan Guo, Tom Goldstein, Awni Hannun, and Laurens Van Der Maaten. Certified data removal from machine learning models. *arXiv preprint arXiv:1911.03030*, 2019.
- Varun Gupta, Christopher Jung, Seth Neel, Aaron Roth, Saeed Sharifi-Malvajerdi, and Chris Waites. Adaptive machine unlearning. *Advances in Neural Information Processing Systems*, 34:16319–16330, 2021.
- Kaiming He, Xiangyu Zhang, Shaoqing Ren, and Jian Sun. Deep residual learning for image recognition. In *CVPR*, pp. 770–778, 2016.
- Dan Hendrycks and Thomas Dietterich. Benchmarking neural network robustness to common corruptions and perturbations. In *International Conference on Learning Representations*, 2019.
- Dan Hendrycks, Steven Basart, Norman Mu, Saurav Kadavath, Frank Wang, Evan Dorundo, Rahul Desai, Tyler Zhu, Samyak Parajuli, Mike Guo, et al. The many faces of robustness: A critical analysis of out-of-distribution generalization. In *Proceedings of the IEEE/CVF international conference on computer vision*, pp. 8340–8349, 2021.
- Chris Jay Hoofnagle, Bart Van Der Sloot, and Frederik Zuiderveen Borgesius. The european union general data protection regulation: what it is and what it means. *Information & Communications Technology Law*, 28(1):65–98, 2019.
- Mir Rayat Imtiaz Hossain, Mennatullah Siam, Leonid Sigal, and James J Little. Visual prompting for generalized few-shot segmentation: A multi-scale approach. In *Proceedings of the IEEE/CVF Conference on Computer Vision and Pattern Recognition*, pp. 23470–23480, 2024.
- Zhizhong Huang, Jie Chen, Junping Zhang, and Hongming Shan. Learning representation for clustering via prototype scattering and positive sampling. *IEEE Transactions on Pattern Analysis and Machine Intelligence*, 45(6):7509–7524, 2022.
- Gabriel Ilharco, Marco Tulio Ribeiro, Mitchell Wortsman, Suchin Gururangan, Ludwig Schmidt, Hannaneh Hajishirzi, and Ali Farhadi. Editing models with task arithmetic. *arXiv preprint arXiv:2212.04089*, 2022.
- Zachary Izzo, Mary Anne Smart, Kamalika Chaudhuri, and James Zou. Approximate data deletion from machine learning models. In *International Conference on Artificial Intelligence and Statistics*, pp. 2008–2016. PMLR, 2021.
- Jinghan Jia, Jiancheng Liu, Parikshit Ram, Yuguang Yao, Gaowen Liu, Yang Liu, Pranay Sharma, and Sijia Liu. Model sparsity can simplify machine unlearning. *Advances in neural information processing systems*, 36, 2023.
- Menglin Jia, Luming Tang, Bor-Chun Chen, Claire Cardie, Serge Belongie, Bharath Hariharan, and Ser-Nam Lim. Visual prompt tuning. In *European Conference on Computer Vision*, pp. 709–727. Springer, 2022.

- Alex Krizhevsky, Geoffrey Hinton, et al. Learning multiple layers of features from tiny images. 2009.
- Meghdad Kurmanji, Eleni Triantafillou, and Peter Triantafillou. Machine unlearning in learned databases: An experimental analysis. *Proceedings of the ACM on Management of Data*, 2(1):1–26, 2024a.
- Meghdad Kurmanji, Peter Triantafillou, Jamie Hayes, and Eleni Triantafillou. Towards unbounded machine unlearning. *Advances in neural information processing systems*, 36, 2024b.
- Guihong Li, Hsiang Hsu, Chun-Fu Chen, and Radu Marculescu. Machine unlearning for image-to-image generative models. *arXiv preprint arXiv:2402.00351*, 2024a.
- Xunkai Li, Yulin Zhao, Zhengyu Wu, Wentao Zhang, Rong-Hua Li, and Guoren Wang. Towards effective and general graph unlearning via mutual evolution. In *Proceedings of the AAAI Conference on Artificial Intelligence*, volume 38, pp. 13682–13690, 2024b.
- Shen Lin, Xiaoyu Zhang, Chenyang Chen, Xiaofeng Chen, and Willy Susilo. Erm-ktp: Knowledge-level machine unlearning via knowledge transfer. In *Proceedings of the IEEE/CVF Conference on Computer Vision and Pattern Recognition*, pp. 20147–20155, 2023.
- Jiancheng Liu, Parikshit Ram, Yuguang Yao, Gaowen Liu, Yang Liu, PRANAY SHARMA, Sijia Liu, et al. Model sparsity can simplify machine unlearning. *Advances in Neural Information Processing Systems*, 36, 2024a.
- Sijia Liu, Yuanshun Yao, Jinghan Jia, Stephen Casper, Nathalie Baracaldo, Peter Hase, Xiaojun Xu, Yuguang Yao, Hang Li, Kush R Varshney, et al. Rethinking machine unlearning for large language models. *arXiv preprint arXiv:2402.08787*, 2024b.
- Weihuang Liu, Xi Shen, Chi-Man Pun, and Xiaodong Cun. Explicit visual prompting for low-level structure segmentations. In *Proceedings of the IEEE/CVF Conference on Computer Vision and Pattern Recognition*, pp. 19434–19445, 2023.
- Aleksander Madry, Aleksandar Makelov, Ludwig Schmidt, Dimitris Tsipras, and Adrian Vladu. Towards deep learning models resistant to adversarial attacks. *arXiv preprint arXiv:1706.06083*, 2017.
- Igor Melnyk, Vijil Chenthamarakshan, Pin-Yu Chen, Payel Das, Amit Dhurandhar, Inkit Padhi, and Devleena Das. Reprogramming pretrained language models for antibody sequence infilling. In *International Conference on Machine Learning*, pp. 24398–24419. PMLR, 2023.
- Changdae Oh, Hyeji Hwang, Hee-young Lee, YongTaek Lim, Geunyoung Jung, Jiyoung Jung, Hosik Choi, and Kyungwoo Song. Blackvip: Black-box visual prompting for robust transfer learning. In *Proceedings of the IEEE/CVF Conference on Computer Vision and Pattern Recognition*, pp. 24224–24235, 2023.
- Chao Pan, Jin Sima, Saurav Prakash, Vishal Rana, and Olgica Milenkovic. Machine unlearning of federated clusters. *arXiv preprint arXiv:2210.16424*, 2022.
- Vasileios Perifanis, Efstathios Karypidis, Nikos Komodakis, and Pavlos Efraimidis. Sftc: Machine unlearning via selective fine-tuning and targeted confusion. In *European Interdisciplinary Cybersecurity Conference*, pp. 29–36, 2024.
- Nicholas Pochinkov and Nandi Schoots. Dissecting language models: Machine unlearning via selective pruning. *arXiv preprint arXiv:2403.01267*, 2024.
- Samuele Poppi, Sara Sarto, Marcella Cornia, Lorenzo Baraldi, and Rita Cucchiara. Multi-class explainable unlearning for image classification via weight filtering. *arXiv preprint arXiv:2304.02049*, 2023.
- Weijia Shi, Jaechan Lee, Yangsibo Huang, Sadhika Malladi, Jieyu Zhao, Ari Holtzman, Daogao Liu, Luke Zettlemoyer, Noah A Smith, and Chiyuan Zhang. Muse: Machine unlearning six-way evaluation for language models. *arXiv preprint arXiv:2407.06460*, 2024.
- Karen Simonyan and Andrew Zisserman. Very deep convolutional networks for large-scale image recognition. *arXiv preprint arXiv:1409.1556*, 2014.
- Jafar Tahmoresnezhad and Sattar Hashemi. Visual domain adaptation via transfer feature learning. *Knowledge and information systems*, 50:585–605, 2017.
- Yaling Tao, Kentaro Takagi, and Kouta Nakata. Clustering-friendly representation learning via instance discrimination and feature decorrelation. *arXiv preprint arXiv:2106.00131*, 2021.
- Anvith Thudi, Gabriel Deza, Varun Chandrasekaran, and Nicolas Papernot. Unrolling sgd: Understanding factors influencing machine unlearning. In *2022 IEEE 7th European Symposium on Security and Privacy (EuroS&P)*, pp. 303–319. IEEE, 2022a.
- Anvith Thudi, Hengrui Jia, Iliia Shumailov, and Nicolas Papernot. On the necessity of auditable algorithmic definitions for machine unlearning. In *31st USENIX Security Symposium (USENIX Security 22)*, pp. 4007–4022, 2022b.

- Yun-Yun Tsai, Pin-Yu Chen, and Tsung-Yi Ho. Transfer learning without knowing: Reprogramming black-box machine learning models with scarce data and limited resources. In *International Conference on Machine Learning*, pp. 9614–9624. PMLR, 2020.
- Jindong Wang, Wenjie Feng, Yiqiang Chen, Han Yu, Meiyu Huang, and Philip S Yu. Visual domain adaptation with manifold embedded distribution alignment. In *Proceedings of the 26th ACM international conference on Multimedia*, pp. 402–410, 2018.
- Lingzhi Wang, Tong Chen, Wei Yuan, Xingshan Zeng, Kam-Fai Wong, and Hongzhi Yin. Kga: A general machine unlearning framework based on knowledge gap alignment. *arXiv preprint arXiv:2305.06535*, 2023a.
- Lingzhi Wang, Xingshan Zeng, Jinsong Guo, Kam-Fai Wong, and Georg Gottlob. Selective forgetting: Advancing machine unlearning techniques and evaluation in language models. *arXiv preprint arXiv:2402.05813*, 2024a.
- Weiqi Wang, Zhiyi Tian, Chenhan Zhang, and Shui Yu. Machine unlearning: A comprehensive survey. *arXiv preprint arXiv:2405.07406*, 2024b.
- Wenhao Wang, Yifan Sun, Wei Li, and Yi Yang. Transhp: Image classification with hierarchical prompting. *Advances in Neural Information Processing Systems*, 36:28187–28200, 2023b.
- Alexander Warnecke, Lukas Pirch, Christian Wressnegger, and Konrad Rieck. Machine unlearning of features and labels. *arXiv preprint arXiv:2108.11577*, 2021.
- Chao-Han Huck Yang, Yun-Yun Tsai, and Pin-Yu Chen. Voice2series: Reprogramming acoustic models for time series classification. In *International conference on machine learning*, pp. 11808–11819. PMLR, 2021.
- Guanhua Zhang, Yihua Zhang, Yang Zhang, Wenqi Fan, Qing Li, Sijia Liu, and Shiyu Chang. Fairness reprogramming. *Advances in Neural Information Processing Systems*, 35:34347–34362, 2022.
- Yichi Zhang, Yinpeng Dong, Siyuan Zhang, Tianzan Min, Hang Su, and Jun Zhu. Exploring the transferability of visual prompting for multimodal large language models. In *Proceedings of the IEEE/CVF Conference on Computer Vision and Pattern Recognition*, pp. 26562–26572, 2024a.
- Yimeng Zhang, Xin Chen, Jinghan Jia, Yihua Zhang, Chongyu Fan, Jiancheng Liu, Mingyi Hong, Ke Ding, and Sijia Liu. Defensive unlearning with adversarial training for robust concept erasure in diffusion models. *arXiv preprint arXiv:2405.15234*, 2024b.

Appendix

A Generalization of MU to Forget Data Shifts

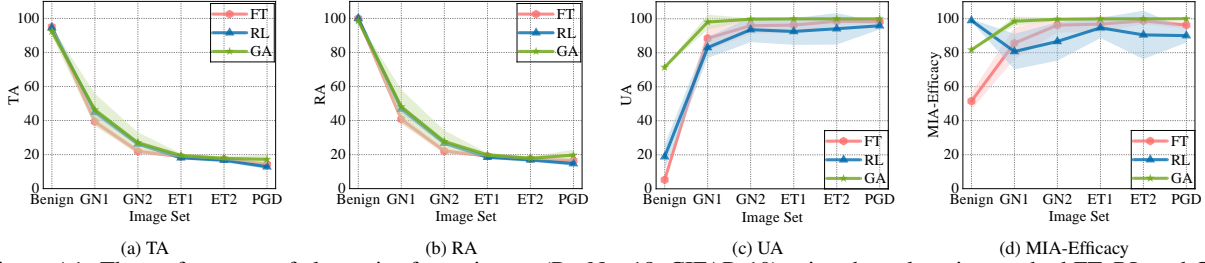


Figure A1: The performance of class-wise forgetting on (ResNet-18, CIFAR-10) using the unlearning method FT, RL and GA, evaluated on both benign evaluation sets (Benign) and perturbed sets, which include (1) Gaussian noise (GN) with a standard deviation of 0.08 (termed GN1), (2) GN with a standard deviation of 0.2 (termed GN2), (3) Elastic transformation (ET) with parameters (488, 170.8, 24.4) regarding intensity, smoothing, and offset (termed ET1), (4) ET with parameters (488, 19.52, 48.8) (termed ET2), and (5) adversarial perturbations from a 7-step PGD attack with strength $\epsilon = 8/255$. The unlearning performance metrics are reported as (a) TA (testing accuracy), (b) RA (retain accuracy), (c) UA (unlearning accuracy), and (d) MIA-Efficacy, as defined in Sec.3 of main paper. The average performance is reported over 10 independent trials, where each trial focuses on forgetting one specific class from CIFAR-10. Shaded regions indicate the performance variance.

In **Fig. A1**, we provide additional evaluations of other approximate unlearning methods, including FT, RL, and GA against Gaussian noise at test time with standard deviations of 0.08 and 0.2 (Hendrycks & Dietterich, 2019), and two types of Elastic transformations with parameters (488, 170.8, 24.4) and (488, 19.52, 48.8) regarding intensity, smoothing and offset for moderate and high-intensity distortions (Hendrycks & Dietterich, 2019), as well as a 7-step PGD attack with perturbation strength $\epsilon = 8/255$ (Goodfellow et al., 2014). The experiments are conducted on the CIFAR-10 dataset using ResNet-18 for the image classification task. As can be seen, the experimental results presented in **Fig. A1** are consistent with the findings in Sec.4 of the main paper, further reinforcing the validity of our conclusions. Specifically, as shown in **Fig. A1**-(a) and (b), model utility, measured by RA (retain accuracy) and TA (testing accuracy), decreases when external perturbations are applied to the evaluation sets compared to its original performance without perturbations. Meanwhile, **Fig. A1**-(c) and (d) show that unlearning effectiveness measured by UA (unlearning accuracy) and MIA-Efficacy, remains stable despite the presence of these perturbations on the forget set.

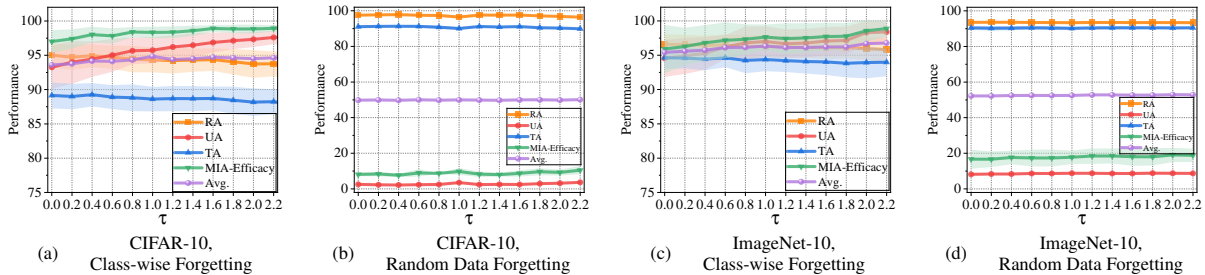
B Parameter Sensitivity Analysis: Prediction Margin τ in Forget Vector Loss

Figure A2: Sensitivity analysis of the nonnegative margin parameter τ for image classification under two unlearning scenarios on CIFAR-10 and ImageNet-10 using ResNet-18 and VGG-16, respectively. The unlearning performance metrics are reported as (a) TA (testing accuracy, blue curve), (b) RA (retain accuracy, orange curve), (c) UA (unlearning accuracy, red curve), and (d) MIA-Efficacy (green curve), (e) the average (Avg.) performance across TA, RA, UA, and MIA-Efficacy (purple curve). For class-wise forgetting scenario, the performance is averaged over 10 independent trials, with each trial focusing on forgetting one specific class from the dataset. Similarly, for random-data forgetting scenario, the performance is reported across 10 independent trials, where each trial targets the forgetting of a random subset of the dataset. The shaded regions represent the variance in performance across trials.

In **Fig. A2**, we provide the sensitivity analysis of τ on two datasets regarding two forgetting scenarios: class-wise forgetting and random data forgetting, where we varied τ from 0.0 to 2.2 with a step of 0.2. As can be seen, the forget objective is robust to variations in the nonnegative margin parameter τ . When τ is set to 1, the performance across four metrics achieves an optimal tradeoff. Therefore, we choose $\tau = 1$ for our experiments.

C Ablation Studies

C.1 Component Analysis: λ_1 and λ_2

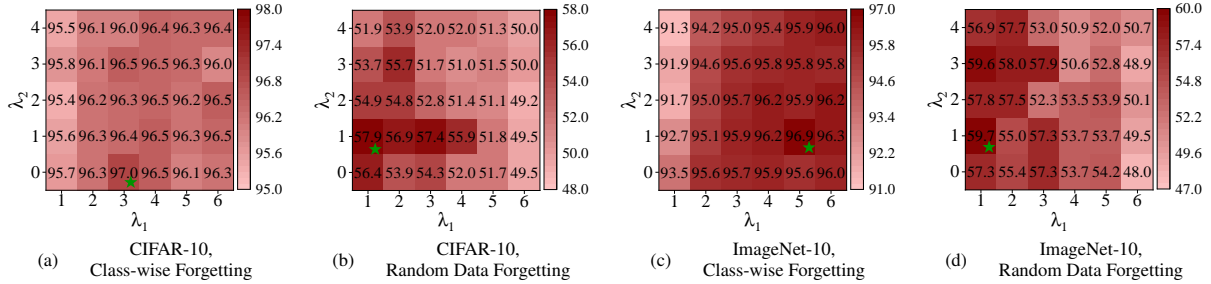


Figure A3: Sensitivity analysis of the nonnegative hyper-parameters λ_1 (ranging from 1 to 5 with an interval of 1) and λ_2 (ranging from 0 to 4 with an interval of 1) for image classification under two unlearning scenarios on CIFAR-10 and ImageNet-10 using ResNet-18 and VGG-16, respectively. The unlearning performance is reported using *the average (avg.) performance across UA, RA, TA, and MIA-Efficacy*, with a green star (★) marking the chosen parameter scheme (λ_1 and λ_2) in our experiments. The color bar on the right represents a gradient scale from light to dark red, indicating the range of values (0 to 100%) in the heatmap. The integer within each cell represents the performance (%) given a combination of λ_1 and λ_2 .

To verify the impact of each key component in the optimization problem (4) of the main paper, we analyze the nonnegative trade-off parameters λ_1 and λ_2 in **Fig. A3**. As can be seen in **Fig. A3**-(a) and (c), setting the retain loss regularization parameter λ_1 to 3 for CIFAR-10 and 5 for ImageNet-10 in class-wise forgetting, along with the ℓ_2 -norm regularization parameter $\lambda_2 = 1$, enables our proposed method to achieve the highest average performance. Meanwhile, for the random data forgetting scenario, setting both λ_1 and λ_2 to 1 yields the best average performance for CIFAR-10 and ImageNet-10.

C.2 Run-time Efficiency

Table A1: The computational efficiency overview of various MU methods for image classification under two unlearning scenarios on CIFAR-10 and ImageNet-10 using ResNet-18 and VGG-16, respectively. Results are reported in terms of RTE (run-time efficiency) measured in *minutes* for the overall training phase.

MU Method	CIFAR-10		ImageNet-10	
	Class-wise Forgetting	Random Data Forgetting	Class-wise Forgetting	Random Data Forgetting
Retrain	81.30	103.71	118.89	116.10
FT (Warnecke et al., 2021)	4.56	2.28	2.99	2.95
RL (Golatkhar et al., 2020)	5.61	4.75	3.58	3.59
GA (Thudi et al., 2022a)	1.16	1.15	0.30	0.31
NegGrad+ (Kurmanji et al., 2024a)	4.72	4.22	3.21	3.17
SalUn (Fan et al., 2023)	2.81	3.01	2.56	2.85
SCRUB (Kurmanji et al., 2024b)	1.23	1.53	1.62	1.55
Ours	9.48	10.75	24.60	25.99

To evaluate the computational efficiency in MU, we compare the runtime costs of forget vector calculation with those of other model-based unlearning methods. Following (Fan et al., 2023), we adopt the evaluation metric run-time efficiency (RTE), *i.e.*, the computation time of applying an MU method in minutes. Notably, all evaluations are conducted on the same computational environment utilizing an NVIDIA A6000 GPU, using a consistent batch size across all MU methods to maintain fair and reliable comparisons. The corresponding results can be found in **Tab. A1**. By comparing the training time of model-based methods with our proposed approach, we observe that the forget vector method requires higher computational time than model-based unlearning baselines but remains faster than retraining. This increased time is attributed to the larger number of iterations needed to identify the desired universal input perturbations. However, it is worth noting that the forget vector method optimizes fewer parameters, owing to its input-level design, compared to model-based methods. This trade-off highlights the efficiency of the forget vector in terms of parameter scale despite its higher iteration count.

D Additional Visualization through An Input Saliency Lens

In **Figs. A4** and **A5**, we provide additional visualization results through input saliency map for different methods against forget images and retain images, respectively, using Grad-CAM (Gradient-weighted Class Activation Mapping) (Bengio et al., 2013). Consistent with the main paper, we highlight the salient pixels (*i.e.*, regions most influential to

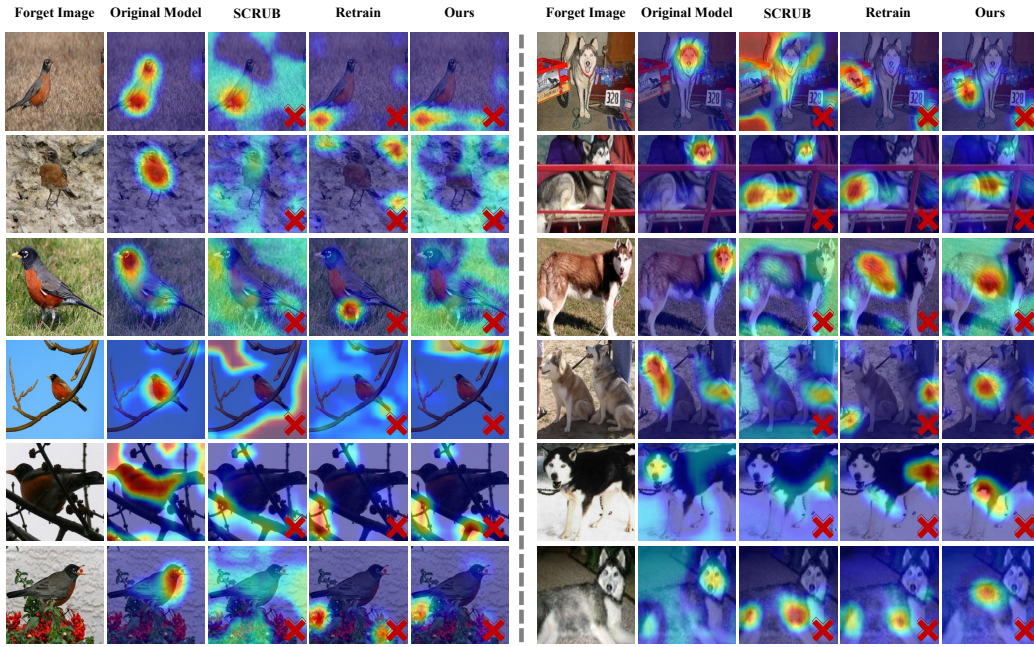


Figure A4: Gradient-based saliency map visualized via Grad-CAM for different MU methods against **forget images**. The highlighted areas (marked in red) indicate regions most influential to model prediction, and the red cross mark (✗) indicates that corresponding methods effectively unlearn the input forget images.

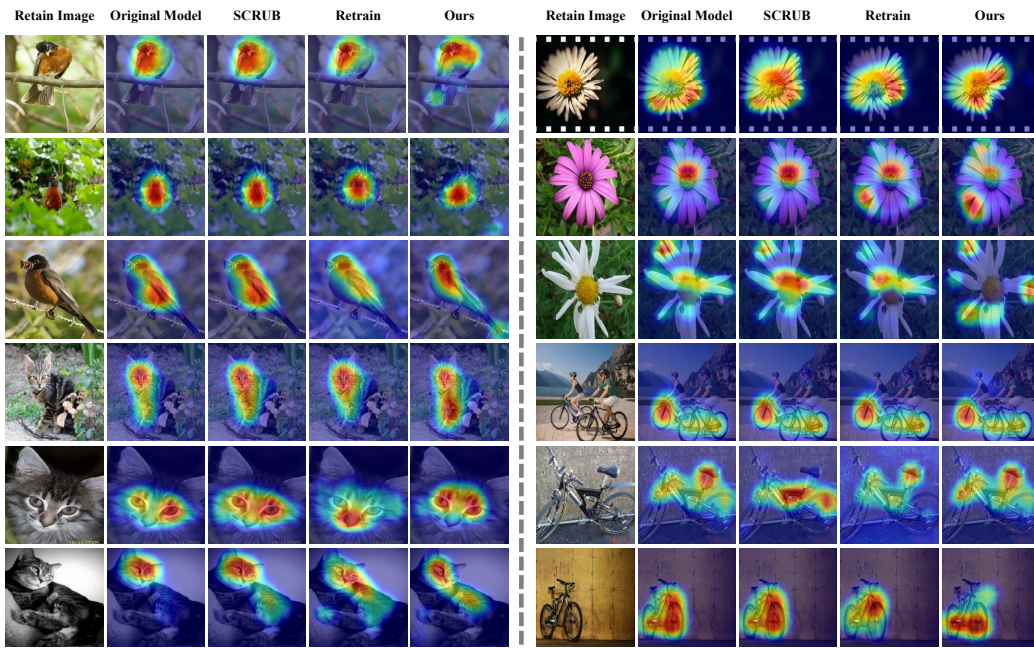


Figure A5: Gradient-based saliency map visualization using Grad-CAM for different MU methods against **retain images**.

model predictions) under four scenarios: (1) the original model (without unlearning), (2) Retrain, (3) SCRUB-based unlearning, and (4) forget vector-based unlearning. For the first three scenarios, saliency maps are generated on raw forget/retain images, whereas for the last scenario, they are applied to images perturbed by the forget vector.